The current issue and full text archive of this journal is available at
www.emeraldinsight.com/0961-5539.htm

Flow over solid blocks in open ended cavity

Effects of blocks' orientations and aspect ratios on the heat transfer rates

S.Z. Shuja, B.S. Yilbas and S.M.A. Khan
ME Department, King Fahd University of Petroleum and Minerals, Dhahran, Saudi Arabia

Received 27 September 2007
Revised 1 July 2008
Accepted 23 September 2008

Abstract

Purpose – The purpose of this paper is to consider flow over heat generating bodies in an open-ends cavity, which finds applications in electronics cooling and industrial processing. Heat transfer rates depend on the flow situation in the cavity, which is influenced by the cavity inlet and exit port locations, heat transferring body size and its orientation in the cavity, and the cavity size. Consequently, modeling of flow over heat transferring bodies in an open-ends cavity and examination of the effect of the aspect ratio and orientation of the heat transferring bodies on the flow field and heat transfer rates becomes essential.

Design/methodology/approach – The flow over heat generating solid blocks situated in an open-ends cavity is considered and the effects of blocks' orientations and aspect ratios on flow field as well as heat transfer rates are examined. A numerical scheme using a control volume approach is introduced to predict flow field in the cavity and heat transfer rates from the blocks.

Findings – It is found that complex flow structure is generated in the cavity due to the aspect ratios and orientations of the blocks. This, in turn, influences significantly heat transfer rates from the blocks in the cavity.

Research limitations/implications – Surface areas of blocks are kept the same and aspect ratio is varied such that the surface area of each block remains the same in the simulations. In addition, Steady flow situation is considered for governing equations of flow and heat transfer in the cavity. However, for the future study transient heating and flow situations can be considered while varying the surface araes of the blocks. This will provide useful information on the circulations in the cavity and the enhancement of heat transfer due to the complex flow structure.

Practical implications – In practice, cooling effectiveness can be improved through changing the aspects ratio of the heat generating bodies in the cavity.

Originality/value – The findings are original and will be useful for the scientists and the design engineers working the specific area of heat transfer and fluid flow.

Keywords Heat transfer, Flow, Blocks

Paper type Research paper

Nomenclature

a	= aspect ratio	Gr	= Grashof number
b	= length of solid body (m)	h	= heat transfer coefficient (W/m^{2}K)
c	= height of solid body (m)	k	= thermal conductivity (W/mK)
Cp	= specific heat capacity (J/kgK)	L	= cavity length (m)
		Nu	= Nusselt number

Acknowledgments are due to King Fahd University of Petroleum and Minerals.

International Journal of Numerical Methods for Heat & Fluid Flow
Vol. 19 No. 5, 2009
pp. 633-649

0961-5539
DOI 10.1108/09615530910963562

P = pressure (Pa)
T = temperature (K)
Ti = temperature at cavity inlet (K)
u = velocity in x-axis (m)
v = velocity in y-axis (m)
V = velocity magnitude (m/s)
Vi = velocity magnitude at cavity inlet (m/s)
w = size of the solid body (m)
x = distance in x-axis (m)
y = distance in y-axis (m)

Greek symbols

α = thermal diffusivity (m^2/s)
β = expansion coefficient (K^{-1})
φ = any flow variable
μ = dynamic viscosity ($N.s/m^3$)
υ = kinematic viscosity (m^2/s)
ρ = density (kg/m^3)

1. Introduction

Flow over heat generating bodies in an open-ends cavity finds applications in electronics cooling and industrial processing. Heat transfer rates depend on the flow situation in the cavity, which is influenced by the cavity inlet and exit port locations, heat transferring body size and its orientation in the cavity and the cavity size. Moreover, proper selection of the geometric and flow parameters results in improved heat transfer rates from the body in the cavity. Model studies provide insight in to the flow and heat transfer process, which can be used to minimize the experimental cost and time. Consequently, modeling of flow over heat transferring bodies in an open-ends channel and examination of the effect of the aspect ratio and orientation of the heat transferring bodies on the flow field and heat transfer rates becomes essential.

Considerable research studies were carried out to examine flow in the cavities. Natural convection in a square cavity due to a protruding body and effect of aspect ratio on the heat transfer rates were examined by Shuja *et al.* (2000a). They developed an empirical relation between the Nusselt and the aspect ratio of heat transferring body and showed that increasing aspect ratio reduced the Nusselt number. Flow structure due to dimple depressions on a channel surface was examined by Ligrani *et al.* (2001). They showed that the locations of the primary and secondary vortex pairs near the dimpled surface coincided closely with locations where normalized Reynolds stress was augmented. Mixed convection in a narrow rectangular cavity with bottom inlet and outlet was studied by Rosengarten *et al.* (2001). He showed that the mean Nusselt number was independent of buoyancy forces when the stratification correction parameter was taken into account. Natural convection in a two-dimensional enclosure heated symmetrically from both sides was examined by Das *et al.* (2002). They indicated that numerical prediction of flow field agreed well with the experimental results obtained from the visualization tests. Mixed convection heat transfer in two-dimensional open-ends enclosures was considered by Khanafer *et al.* (2002). They showed that thermal insulation of the cavity could be achieved through the use of high velocity horizontal flow. Local heat transfer characteristics in electronics modules were studied by Yoo *et al.* (2003). They indicated that longitudinal vortices formed by vortex generator enhanced the mixing of fluids and thereby heat transfer, and the rectangular wing type vortex generator was found to be more effective that the delta wing type vortex generator. The conjugate heat transfer in inclined open shallow cavities was carried out by Polat and Bilgen (2003). They indicated that the Nusselt number was an

increasing function of the aspect ratio up to a critical Rayleigh number. Mixed convection in rectangular enclosures with adiabatic fins attached on the heated wall was examined by Kasbioui *et al.* (2003). They showed that for critical values of the Reynolds and Rayleigh numbers, heat transfer rates became maximum of which the value was independent of the aspect ratio when the aspect ratio becomes greater than or equal to 10. Mixed convection in two-sided lid-driven differentially heated square cavity was studied by Oztop and Dagtekin (2004). They indicated that for the case of opposing buoyancy and shear forces and for Richardson number greater than 1, heat transfer rates improved because of the secondary cells near the walls and a counter rotating cell at the center. Mixed convection from an open cavity in a horizontal channel was examined by Leong *et al.* (2005). They indicated that in the mixed convection regime, heat transfer rate is reduced and flow became unstable. Natural convection of air in tall vertical cavity was studied by Wright *et al.* (2006). They showed that most of the temperature drop existed in the boundary layers near the walls and the cone was well mixed and of relatively uniform temperature with little or no vertical stratification. Numerical simulation of two-dimensional laminar mixed convection in a lid-driven cavity was carried out by Wong (2007). He proposed a mixed finite element method using the consistent splitting scheme. Iwatsu *et al.* (1993) examined flow and heat transfer of a viscous fluid contained in a square cavity. They imposed the vertical temperature gradient on the system boundaries in the numerical simulations. The effects of sharp corners on buoyancy-driven flows were investigated by Vafai and Etterfagh (1990). They analyzed the transient behavior of the flow field through the formation of vortices and the opposing interactions of the buoyant and suction mechanisms leading to an oscillating central vortex. Khanafer and Vafai (2002) examined the buoyancy-driven flow and heat transfer in open-ended enclosures. The work presented constituted an innovative way for describing correctly the boundary conditions at the open side of an open-ended boundary. The mixed convection heat transfer in a rectangular cavity ventilated and heated from the side was investigated by Raji and Hasnaoui (1998). They proposed useful correlations for the heat transfer rates and the Rayleigh as well as the Reynolds numbers. The linear stability of flow in a differential heated cavity via large-scale eigenvalue calculations was examined by Burroughs *et al.* (2004). They indicated that due to the symmetry of the problem, the first two unstable modes would have eigenvalues, which were nearly identical, and the numerical simulations confirmed this situation. The natural convection in a shallow rectangular cavity filled with non-Newtonian fluid and heated from all sides was investigated by Lamsaadi *et al.* (2006). They showed that the flow field and heat transfer were sensitive to the non-Newtonian behavior of the fluid. The effect of viscous dissipation on mixed flow in a rectangular enclosure with isothermal wall was examined by Hossain and Gorla (2006). They indicated that the effect of viscous dissipation was to increase the fluid temperature and resulted in the formation of vortex motion near the lower part of the cavity in an opposite direction to the central vortex. The natural convection and heat transfer in a square cavity with large horizontal temperature differences was studied by Vierendeels *et al.* (2003). The heat transfer rates were determined for various Rayleigh numbers and temperature differences. The mixed convection in a square cavity due to heat generating rectangular body was investigated by Shuja *et al.* (2000b). They showed that non-uniform cooling of the solid body occurred for exit port location numbers 13 and beyond; in which case, heat transfer reduced while irreversibility increased in the cavity. The previous study (Shuja *et al.*, 2000a) was limited with one protruding body in

the cavity and a constant temperature heat source. Therefore, the influence of the second body on the fluid flow and the heat transfer rates in the cavity becomes necessary.

In the present study, flow over heat generating solid blocks situated in an open-ends cavity is considered. In addition, the effects of blocks' orientations and aspect ratios on flow field as well as heat transfer rates are examined. Uniform heat flux is assumed within the blocks and air is used as working fluid. Surface areas of blocks are kept the same and aspect ratio is varied such that the surface area of each block remains the same in the simulations. Steady flow situation is considered for governing equations of flow and heat transfer in the cavity. A numerical scheme using a control volume approach is introduced to predict flow field in the cavity and heat transfer rates from the blocks.

2. Mathematical formulation

Flow around the solid blocks in the square cavity is considered and flow situation is assumed to be incompressible and laminar since the Reynolds number accommodated at present is 100 due to mixed convection situation.

2.1 The flow field

The governing equations are given as follows.

The continuity equation is:

$$\frac{\partial u}{\partial x}+\frac{\partial v}{\partial y}=0 \tag{1}$$

The momentum equation is:

x-momentum

$$u\frac{\partial u}{\partial x}+v\frac{\partial u}{\partial y}=-\frac{1}{\rho_f}\frac{\partial p}{\partial x}+\upsilon\left(\frac{\partial^2 u}{\partial x^2}+\frac{\partial^2 u}{\partial y^2}\right) \tag{2}$$

y-momentum

$$u\frac{\partial v}{\partial x}+v\frac{\partial v}{\partial y}=-\frac{1}{\rho_f}\frac{\partial p}{\partial y}+g\beta\Delta T+\upsilon\left(\frac{\partial^2 v}{\partial x^2}+\frac{\partial^2 v}{\partial y^2}\right) \tag{3}$$

The energy equation is:

$$\rho_f C_{pf}\left(u\frac{\partial T}{\partial x}+v\frac{\partial T}{\partial y}\right)=k_f\left(\frac{\partial^2 T}{\partial x^2}+\frac{\partial^2 T}{\partial y^2}\right)+\mu\phi \tag{4}$$

where

$$\phi=2\left[\left(\frac{\partial u}{\partial x}\right)^2+\left(\frac{\partial v}{\partial y}\right)^2\right]+\left[\frac{\partial v}{\partial x}+\frac{\partial u}{\partial y}\right]^2$$

where ρ_f is the fluid density, k_f is the fluid thermal conductivity and Cp_f is the fluid specific heat capacity.

2.2 The boundary conditions

Figure 1 shows the schematic view of the cavity and the solid blocks for the aspect ratio 2.25, and the boundary conditions as an example.

At solid wall. $u = 0$ and $v = 0$ (no slip and impermeability conditions).

At cavity inlet. At inlet port of the cavity a uniform fluid temperature ($T_{inlet} = 300$ K) and uniform flow ($V_i = 0.1216$ m/s) are assumed.

At cavity exit. At exit port of the cavity constant pressure boundary is assumed, since the cavity exit is open to the free atmosphere. However, mass continuity should be satisfied at the cavity exit, which results $(V_{average})_{exit} = 0.1216$ m/s. In the case of the back flow situation at the cavity exit, temperature is set at $T_{exit} = 300$ K. The back flow situation was checked through setting the second derivatives of velocity and temperature as zero at the cavity exit. The velocity distribution at the cavity exit is shown in Figure 2. It is evident from Figure 2 that the back flow does not occur.

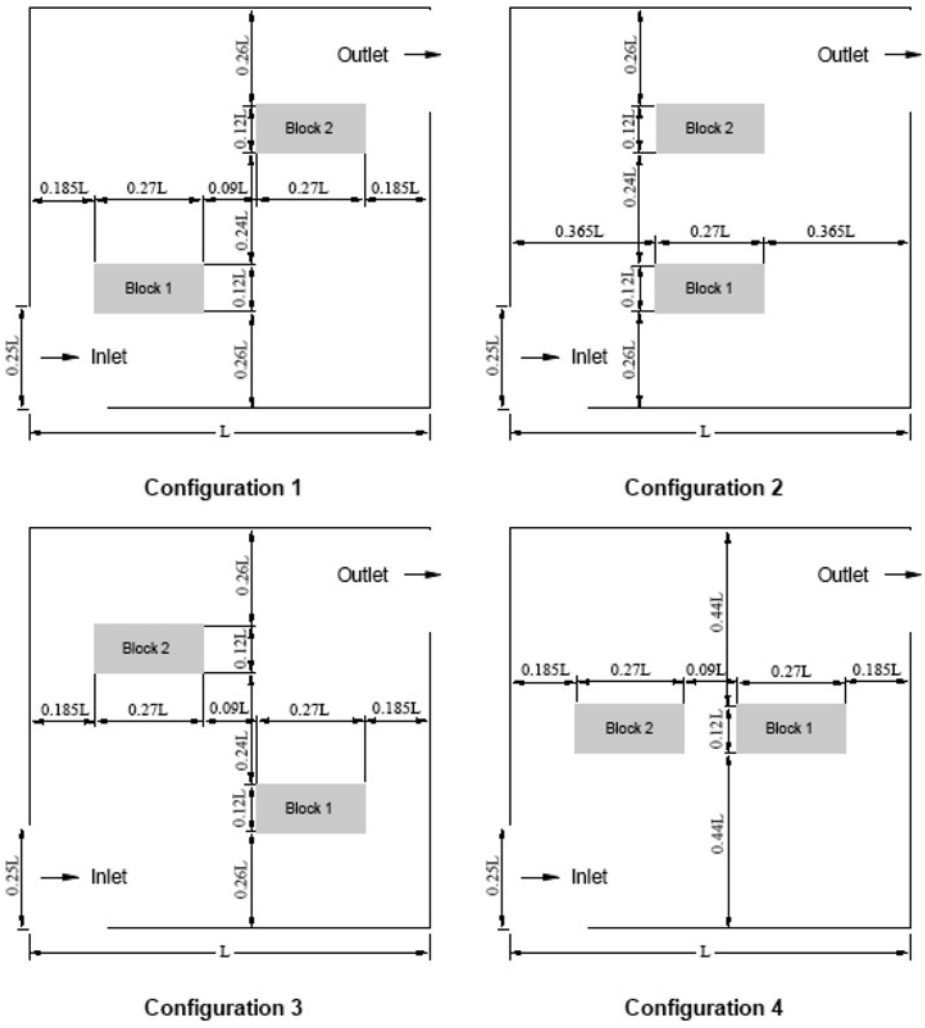

Figure 1.
View of cavity and solid blocks in the cavity. Blocks configurations in the cavity for the block aspect ratio of 2.25 and L = 0.05 m

At cavity wall. The cavity walls are considered to be adiabatic (no heat transfer to the cavity outer environment) and no slip and impermeability conditions are adopted for the flow (u = 0 and v = 0).

2.3 The solid blocks

The energy equation is:

$$0 = k_s\left(\frac{\partial^2 T}{\partial x^2} + \frac{\partial^2 T}{\partial y^2}\right) + \dot{q}''' \tag{5}$$

where ρ_s is the solid density, k_s is the solid thermal conductivity, and Cp_s is the solid specific heat capacity, and $\dot{q}'''$ is the volumetric heat generation per unit time (power input) over the body.

Boundary conditions. At the solid walls of the blocks:

$$-k\frac{\partial T}{\partial n} = h(T_w - T_i);\ T_s = T_f \quad \text{and} \quad \dot{q}''' = 1 \times 10^5\ W/m^3.$$

The value of $\dot{q}'''$ is selected in line with the heat generation by the electronic device such as Pentium IV process (Yu and Harvey, 2003). T_w is temperature at the solid wall and T_i is temperature at the cavity inlet. The dimensionless numbers used in the analysis are the Nusselt and Grashof numbers. The Nusselt number is $Nu = (hw/k_f)$ where $h = (-k\partial T/\partial n)_{wall}/(T_w - T_i)$, w is the size of the block (side length of the block = 0.12 L), and n is the direction normal to the surface. The averaged heat transfer coefficient is determined from (Oztop and Dagtakin, 2004): $\bar{h} = (1/w_{tot})\int_{Perimeter} h d\eta$, where w_{tot} is the perimeter of the solid block and η is the length scale around perimeter of the solid block. The Grashof number is $Gr = (g\beta\Delta T w^3)/(\nu^2)$ ($\Delta T = (T_{av} - T_i)$, where T_{av} is the average temperature of the solid block). The Reynolds number is defined at the cavity inlet, i.e. $Re = (V_i l)/(\nu)$, where V_i (0.1216 m/s) is the velocity at the cavity inlet, l (0.0125 m) is the cavity inlet

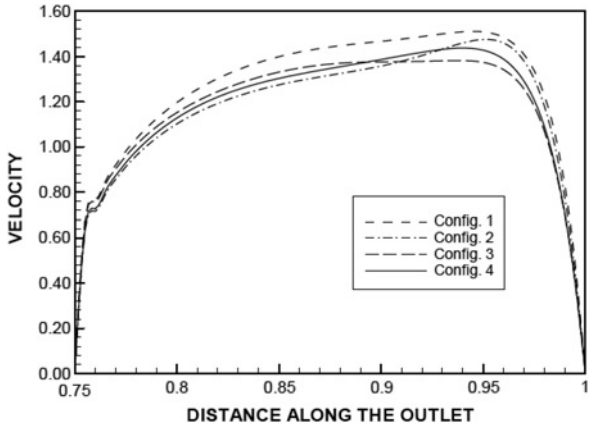

Figure 2.
Normalized velocity (V/Vi, where Vi is velocity magnitude at the cavity inlet) along the normalized outlet (Distance Along Cavity Depth/0.25×L, where L is the cavity length L = 0.05 m) for four configurations

port height, and ν (1.52×10^{-5} m^2/s) is the kinematic viscosity. In the simulations, the Reynolds number is kept as 100.

The aspect ratio of the protruding body is determined in accordance with the cavity size, which is shown in Figures 1 and 2. The size of the protruding body can be formulated as:

$$b = 0.18\frac{L}{\sqrt{a}} \quad \text{and} \quad c = 0.18\sqrt{a}L$$

where b and c are length and height of the protruding body, and L is the cavity length. In the simulations, L is selected as 0.05 m in relation to the electronic device cooling in control units. Knowing the aspect ratio "a" the size of the protruding body can be determined. It should be noted that the area of the protruding body is kept constant for all aspect ratios, i.e: Area = b.c (= constant).

2.4 Numerical solution

The flow domain is overlaid with a rectangular grid and the grid used in the present study has 100×100 node points. The control volume approach is employed in the numerical scheme. All the variables are computed at each grid point except the velocities, which are determined midway between the grid points. The grid independent tests are conducted. Table I gives the grid independent test results. The Richardson number is tabulated for different grid sizes used in the grid independent tests. It can be observed that the Richardson number remains similar when the grid size is increased 20 percent more and less than the grid size of 200×200. Therefore, the grid size of 200×200 grid points is selected on the basis of less computation time without compromising the grid independence. The power law difference scheme is used for convection terms while central difference scheme is adopted for the diffusion terms (Yu and Harvey, 2000). The convergence criterion for the residuals is set as $|\psi^k - \psi^{k-1}| \leq 10^{-6}$ to terminate the simulations. Moreover, in the simulations, the relaxation factors adopted are 0.3 for the continuity equation, 0.7 for the momentum equation, and 1 for the energy equation. The relaxation factors are kept the same for all the numerical simulations. The total number of iteration to secure the converge results while using the workstation DELL Precision 670 (xeon processor) is 1,800.

A staggered grid arrangement is used in the present study, which provides the pressure linkages through the continuity equation and is known as SIMPLEC algorithm (Chung, 2002). This procedure is an iterative process for convergence. The pressure link between continuity and momentum is established by transforming the continuity equation into a Poisson equation for pressure. The Poisson equation implements a pressure correction for a divergent velocity field (Patankar, 1980). The

Grid size	Block 1	Block 2
160×160	80.23	92.49
200×200	81.03	93.03
240×240	81.49	93.38

Note: The simulations are carried out for the configuration 1 (Figures 1 and 2)

Table I. Grid independent tests for the Richardson number (Ri) with different grid sizes

u-velocity correction equation of SIMPLEC algorithm is:

$$u'_{i,J} = (p'_{I-1,J} - p'_{I,J})d_{i,J} \quad \text{where } d_{i,J} = \frac{A_{i,J}}{a_{i,J} - \sum a_{nb}}$$

The v-velocity correction equation of SIMPLEC is:

$$v'_{I,j} = (p'_{I,J-1} - p'_{I,J})d_{I,j} \quad \text{where } d_{I,j} = \frac{A_{I,j}}{a_{I,j} - \sum a_{nb}}$$

Moreover, the discretised pressure equation is the same as in SIMPLE, except that the d-terms are different (Patankar, 1980).

2.5 Model validation

Since the work similar to the geometric configurations of the present work is not found in the open literature. However, mixed convection heat transfer in ventilated cavities reported earlier (Raji and Hasnaoui, 2000) is not appropriate for the model validation due to the non-existing heat generating solid block in the cavity. Therefore, a model study is validated for the square cavity with a protruding heat generating body (Shuja *et al.*, 2001) as similar to the present case. The geometric configurations as well as the relevant flow and the boundary conditions are set the same as those presented in the previous study (Shuja *et al.*, 2001). The heat transfer mechanism is the coupled conduction and natural convection in the square cavity (Shuja *et al.*, 2001). Air is used as the working fluid. The conservation equations for mass continuity, momentum and energy are considered for steady flow. The governing equations are simplified by assuming constant properties and using the Oberbeck-Bossinesque approximation in the y-axis (Shuja *et al.*, 2001). Figure 3 shows the predictions of $Nu/Ra^{0.25}$ with aspect ratio obtained from the present simulations and the previous study. It should be noted that Ra is the Rayleigh number, which is determined from $Ra = (g\beta(T_w - T_i)L^3)/(\upsilon\alpha)$, where β is the thermal expansion coefficient of the working fluid, T_w is the protruding solid body wall temperature, T_i is the reference temperature (fluid temperature at the cavity inlet), L is the length of the square cavity, υ is the kinematic viscosity and α is the thermal diffusivity of the working fluid. It can be

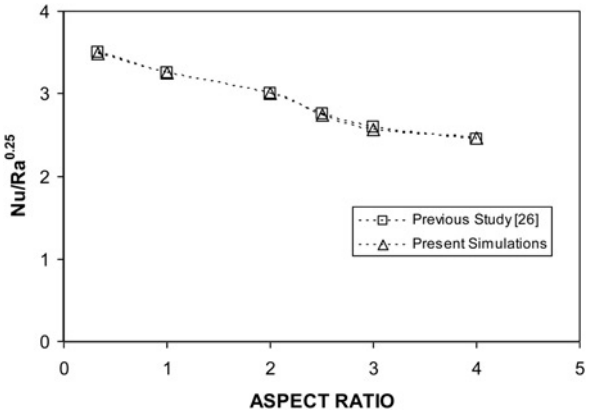

Figure 3.
Model validation for the variation of $Nu/Ra^{0.25}$ with aspect ratio of protruding solid body. The predictions are obtained for the protruding solid body in a square cavity (Raji and Hasnaoui, 2000)

observed from Figure 3 that the predictions and previous results for $Nu/Ra^{0.25}$ with aspect ratios are in good agreement.

3. Results and discussions

Flow over two solid blocks in an open-ends square cavity is considered and flow and temperature fields in the cavity are computed. The effects of block aspect ratio as well as the orientation of solid blocks in the cavity on the flow field and heat transfer rates are examined. Air is used as working fluid in the cavity. Table II gives the fluid and solid properties used in the simulations.

Figure 4 shows stream lines while Figure 5 shows constant velocity lines for three aspect ratios and four configurations of the blocks in the cavity. The velocity magnitude in the figure is normalized (V/V_i) using the velocity at the cavity inlet (V_i). In the case of first configuration, flow passing below the solid bodies in the cavity accelerates through the cavity exit. It should be noted that uniform heat flux in the body generates a thermal boundary layer around the block walls. This, in turn, results in natural convection current, generated by the flow due to the natural convection, in the vicinity of the block surfaces, which is more pronounced at the top surface of the block. Consequently, forced convection and natural convection currents join in the downstream of the block in the region towards the cavity exit. This situation is more pronounced for configurations 1 and 2. Moreover, the effect of the configuration of the blocks in the cavity contributes to flow acceleration below the blocks. In this case, convective cooling of all the surfaces is suppressed. This situation is visible for the aspect ratio of 1/2.25 for all configurations. Moreover, flow splitting in the near upstream of the first block occurs for the configurations 2-4. In this case, blockage effect of the first block results in flow acceleration below the block. However, flow splitting and merging in the cavity causes complicated flow structures, which is influenced significantly by the blocks' configurations and the aspect ratios.

Figure 6 shows isothermal lines in the cavity for different block configurations and the aspect ratios. Temperature is normalized (T/T_i) using the temperature at the cavity inlet (T_i). Contribution of natural convection current to the temperature variation in the cavity is visible for configurations 2 and 3. In this case, mixing of forced and natural convection currents in the downstream of the blocks, results in an extension of high temperature region towards the exit port of the cavity. Thermal boundary layer thickens for the second block for the configurations 1-3. Moreover, due to forced convective current, generated by the flow due to force convection, thermal boundary layer thickness becomes small for configuration 4. Flow acceleration below the blocks in the cavity causes unheated gas flow in this region. Consequently, heated gas is situated in the upper half of the cavity while relatively cool region remains below the blocks in the cavity. Flow spilling around the block results in attainment of low temperature in the vicinity of the block surface. The blockage effect of the blocks in the

	Air	Solid blocks (steel)
Density (Kg/m^3)	1.89	7,836
Specific heat capacity (J/kg K)	1,005	969
Thermal conductivity (W/m K)	0.02565	28.2
Viscosity (m^2/s)	1.544×10^{-5}	

Table II. Properties of air and solid blocks used in the simulations

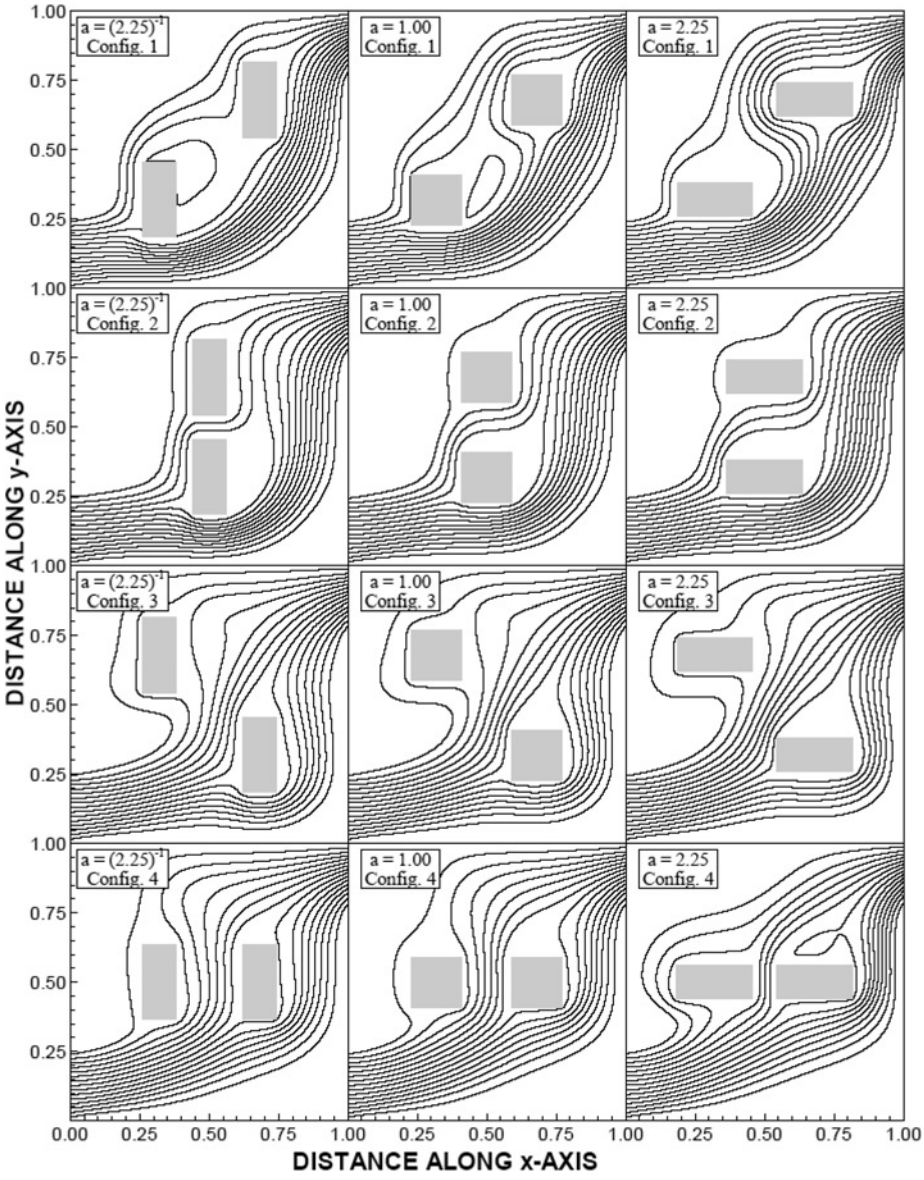

Figure 4.
Stream lines in the cavity for different blocks aspect ratios and configurations

cavity enhances the formation of high temperature around the block. Depending on the configuration, high temperature region extends further in the cavity towards the cavity exit port. Moreover, complex flow structure developed in the cavity causes non-uniform temperature distribution around the blocks, which is more pronounced for configurations 2 and 3.

Figure 7 shows the Nusselt number variation with the aspect ratio for each block at different configurations. In the case of bottom block (Block 1), the Nusselt number attains high values for the low aspect ratio and decays gradually with increasing

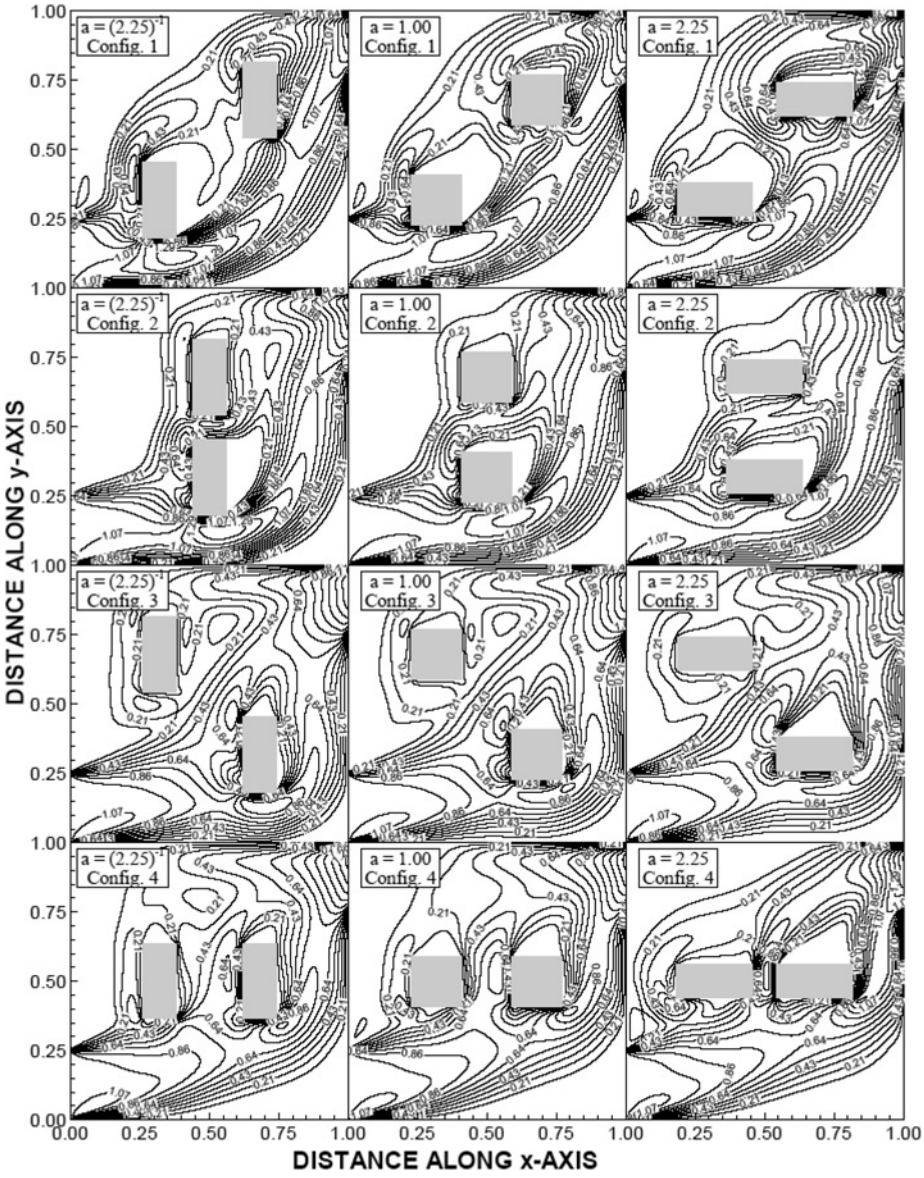

Figure 5.
Normalized constant velocity lines (V/Vi, where Vi is velocity magnitude at the cavity inlet) in the cavity for different blocks aspect ratios and configurations

the aspect ratios for all the configurations, except configuration 4. The gradual decrease in the Nusselt number is because of the cooling rates from the block due to flow structure formed around the bottom block in the cavity. Consequently, thickening of thermal boundary layer and suppression of natural convection current around the block result in attainment of the low Nusselt number. Moreover, the Nusselt number increases for configuration 3; in which case, forced and natural convection currents contribute significantly to thickening of thermal boundary layer around the bottom block. In the case of the top block (Block 2), the Nusselt number attains high values

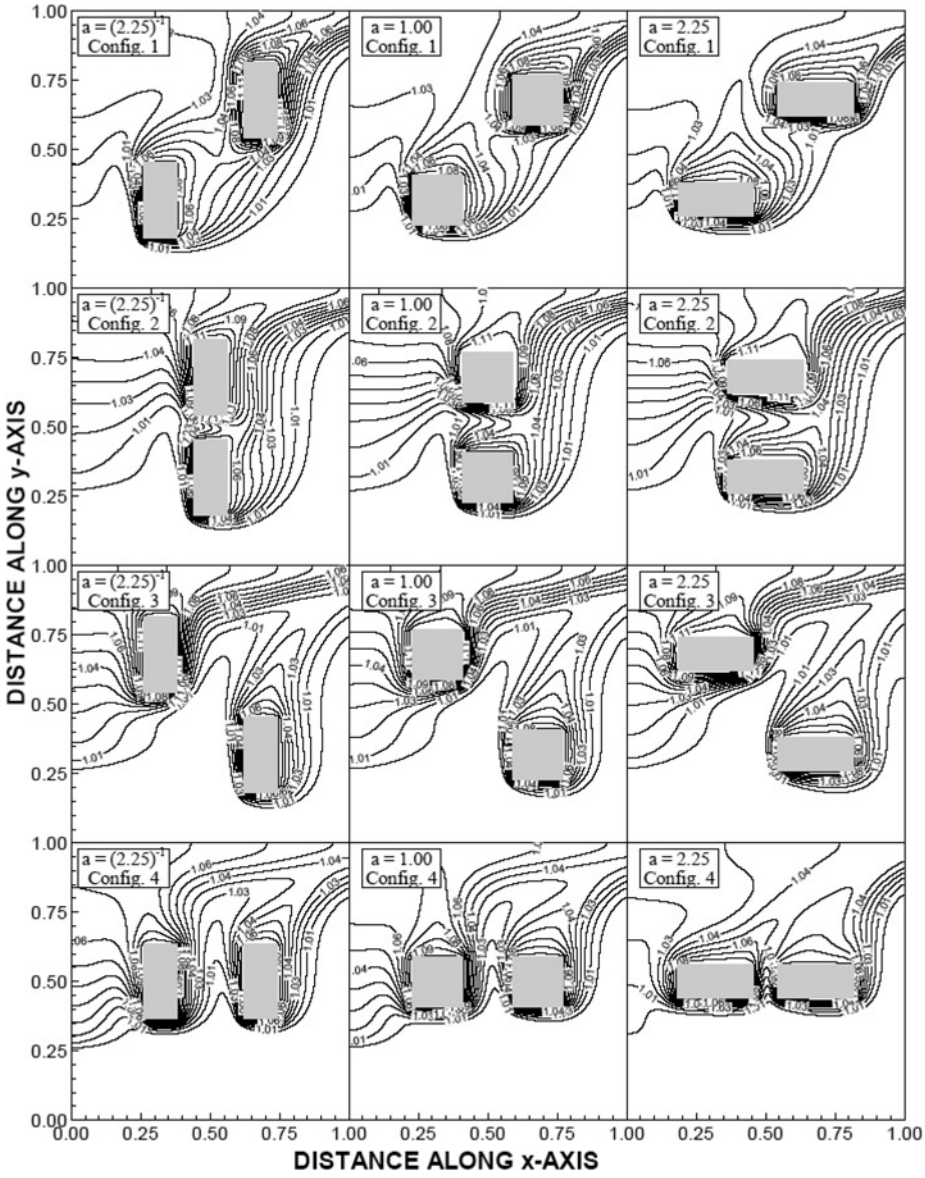

Figure 6.
Normalized isothermal lines (T/Ti, where Ti is temperature at the cavity inlet) in the cavity for different blocks aspect ratios and configurations

for configuration 4 as opposing to the bottom block. Similarly, other configurations result in reverse behavior as discussed for the bottom block. The changes observed in the Nusselt number is associated with the thermal boundary thickness developed around the block in the cavity, i.e. flow spilling and mixing of forced and natural convection currents result in complex flow structure in the cavity affecting the heat transfer rates from the blocks. In general, the Nusselt number attains lower values for the top block than its counterpart corresponding to the bottom block. This argument is true for all the configurations, except configuration 4. This situation can

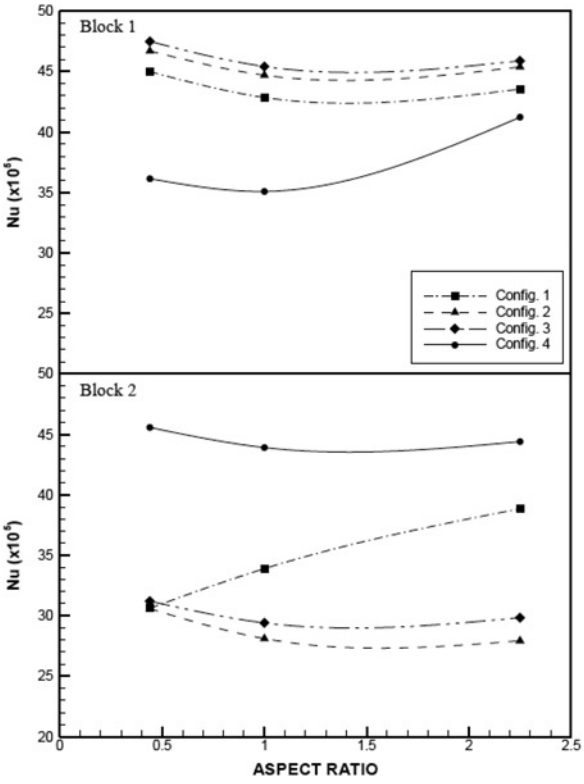

Figure 7.
The variation of Nusselt number predicted with the aspect ratio for each block at different configurations

be explained in terms of location of the inlet and exit ports of the cavity, i.e. forced convective current in the left corner of the block (above the cavity inlet) is small. The effect of aspect ratio on the Nusselt number becomes important for the bottom block for configuration 4 while it is configuration 1 for the top block. Consequently, blocks' orientation and the aspect ratios have coupled effect on the heat transfer rates selectively.

Figure 8 shows the Grashof number variation with the aspect ratio for each block at different configurations. It should be noted that the plot of Grashof number provides information on the ratio of buoyancy force to viscous force; in which case, the buoyancy force is developed mainly due to the natural convection in the cavity. The magnitude of Grashof number varies considerably with the aspect ratio for the bottom block at configuration 4 and for the top block at configuration 1. This variation is similar to the Nusselt number variation, provided that the Grashof number decreases with increasing aspect ratio. Moreover, attainment of the high Grashof number for the bottom block at configuration 4 is because of the thickening of the thermal boundary layer. Moreover, same is true for the top block at configuration 1. The behavior of the Grashof number is opposite to the Nusselt number due to natural convection current contribution to heat transfer rates. The complex flow structure generated in the cavity, due to the orientation and the aspect ratios of the bodies, influences considerably the natural convection current; in which case, the bottom block is affected more from the

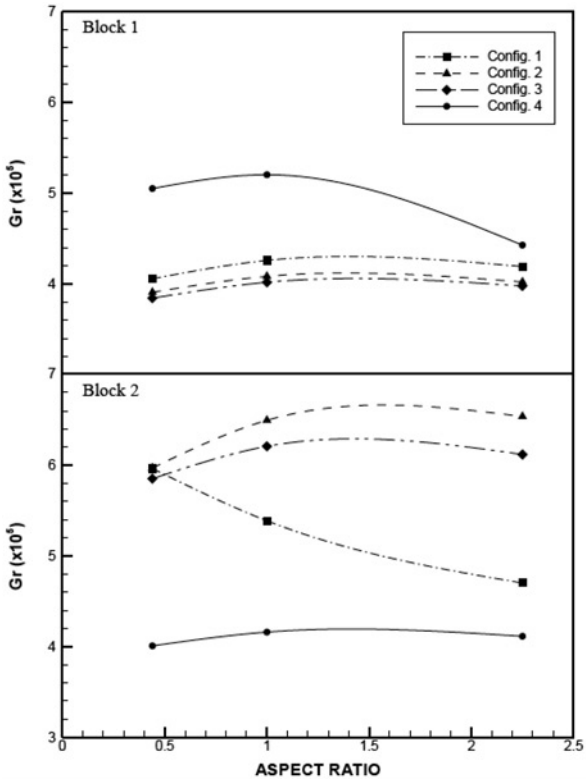

Figure 8.
The variation Grashof number predicted with the aspect ratio for each block at different configurations

forced convection current than the top block. This, in turn, lowers the Grashof number for the bottom block, which is more pronounced for configuration 4.

Figure 9 shows variation of $Nu/Gr^{0.25}$ with the aspect ratio for each block for different configurations. The behavior of curves in the figure is similar to the behavior of the Nusselt number, which is true for both blocks in the cavity. This indicates that the natural convection current for the heat transfer rates from the blocks is less pronounced as compared to the forced convection current.

4. Conclusions

Flow over solid blocks in an open-ended cavity is considered and the effects of blocks' orientations and the aspect ratios on flow field and heat transfer rates are examined. It is found that complex flow structure is developed in the cavity due to flow mixing of forced and natural convective currents and the local acceleration of flow occurs because of the blocks' orientations in the cavity. Consequently, the block aspect ratio and the configuration have significant effect on the thermal boundary layer developed around the blocks. In this case, for certain configurations (such as configuration 1 for the bottom block and configuration 4 for the top block) and aspect ratios (aspect ratio of 1/2.25 for both blocks), the Nusselt number attains high values for both blocks. Therefore, the configuration of the blocks in the cavity resulting in improved heat transfer rates for both blocks is not possible. Moreover, configuration 3 results in relatively improved Nusselt number for both blocks despite the fact that the value of

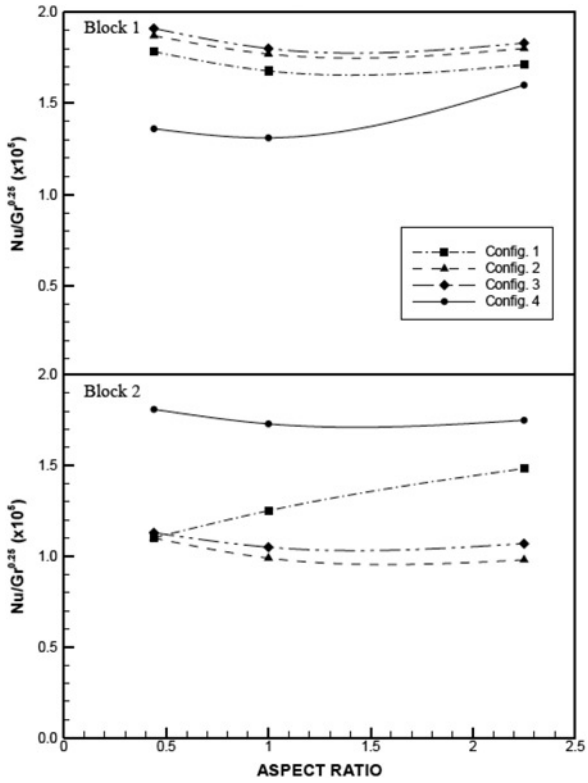

Figure 9.
The variation $Nu/Gr^{0.25}$ predicted with the aspect ratio for each block at different configurations

the Nusselt number is not the maximum for both blocks. In the case of the Grashof number, the opposite behavior is observed than the behavior of the Nusselt number, i.e. the Grashof number increases while the Nusselt number decreases. The ratio of $Nu/Gr^{0.25}$ indicates that the forced convective current has significant effect on cooling rates than that corresponding to the natural convection current.

References

Burrough, E.A., Romero, L.A., Lehoucq, R.B. and Salinger, A.G. (2004), "Linear stability of flow in a differentially heated cavity via large-scale eigenvalue calculations", *International Journal of Numerical Methods for Heat Fluid Flow*, Vol. 14 No. 6, pp. 803-22.

Chung, T.J. (2002), *Computational Fluid Dynamics*, 1st ed., Cambridge University Press, Cambridge.

Das, S.P., Chakraborty, S. and Dutta, P. (2002), "Natural convection in a two-dimensional enclosure heated symmetrically from both sides", *International Communications in Heat and Mass Transfer*, Vol. 29 No. 3, pp. 345-54.

Hossain, Md. A. and Gorla, R.S.R. (2006), "Effect of viscous dissipation on mixed convection flow of water near its density maximum in a rectangular enclosure with isothermal wall", *International Journal of Numerical Methods for Heat Fluid Flow*, Vol. 16 No. 1, pp. 5-17.

Iwatsu, R., Jae Min Hyun and Kuwahara, K. (1993), "Mixed convection in a driven cavity with a stable vertical temperature gradient", *International Journal of Heat and Mass Transfer*, Vol. 36 No. 6, pp. 1601-8.

Kasbioui, S., Lakhal, E.K. and Hasnaoui, M. (2003), "Mixed convection in rectangular enclosures with adiabatic fins attached on the heated wall", *Engineering Computations*, Vol. 20 Nos. 1-2, pp. 152-77.

Khanafer, K. and Vafai, K. (2000), "Buoyancy-driven flow and heat transfer in open-ended enclosures: elimination of the extended boundaries", *International Journal of Heat and Mass Transfer*, Vol. 43, pp. 4087-100.

Khanafer, K., Vafai, K. and Lightstone, M. (2002), "Mixed convection heat transfer in two-dimensional open-ended enclosure", *International Journal of Heat and Mass Transfer*, Vol. 45 No. 26, pp. 5171-90.

Lamsaadi, M., Naimi, M. and Hasnaoui, M. (2006), "Multiple steady state solutions for natural convection in a shallow horizontal rectangular cavity filled with non-Newtonian power-law fluids and heated from all sides", *International Journal of Numerical Methods for Heat Fluid Flow*, Vol. 16 No. 7, pp. 779-802.

Leong, J.C., Brown, N.M. and Lai, F.C. (2005), "Mixed convection from an open cavity in a horizontal channel", *International Communications in Heat and Mass Transfer*, Vol. 32 No. 5, pp. 583-92.

Ligrani, P.M., Harrison, J.L., Mahmmod, G.I. and Hill, M.L. (2001), "Flow structure due to dimple depressions on a channel surface", *Physics of Fluids*, Vol. 13 No. 11, pp. 3442-51.

Oztop, H.F. and Dagtakin, I. (2004), "Mixed convection in two-sided lid-driven differentially heated square cavity", *International Journal of Heat and Mass Transfer*, Vol. 47 Nos. 8-9, pp. 1761-9.

Patankar, S.V. (1980), *Numerical Heat Transfer and Fluid Flow*, Hemisphere, Washington, DC.

Polat, O. and Bilgen, E. (2003), "Conjugate heat transfer in inclined open shallow cavities", *International Journal of Heat and Mass Transfer*, Vol. 46 No. 9, pp. 1563-73.

Raji, A. and Hasnaoui, M. (1998), "Mixed convection heat transfer in a rectangular cavity ventilated and heated from the side", *Numerical Heat Transfer, Part A*, Vol. 33 No. 5, pp. 533-48.

Raji, A. and Hasnaoui, M. (2000), "Mixed convection heat transfer in ventilated cavities with opposing and assisting flows", *Engineering Computations*, Vol. 17 No. 5, pp. 556-72.

Rosengarten, G., Morrison, G.L. and Behnia, M. (2001), "Mixed convection in a narrow rectangular cavity with bottom inlet and outlet", *International Journal of Heat and Fluid Flow*, Vol. 22 No. 2, pp. 168-79.

Shuja, S.Z., Yilbas, B.S. and Iqbal, M.O. (2000a), "Mixed convection in a square cavity due to heat generating rectangular body: effect of cavity exit port locations", *International Journal of Numerical Methods for Heat Fluid Flow*, Vol. 10 No. 8, pp. 824-41.

Shuja, S.Z., Yilbas B.S. and Iqbal, M.O. (2000b), "Heat transfer characteristics of flow past a rectangular protruding body", *Numerical Heat Transfer, Part A*, Vol. 37 No. 3, pp. 307-21.

Shuja, S.Z., Owais, I. and Yilbas, B.S. (2001), "Natural convection in a square cavity due to a protruding body – Aspect ratio consideration", *Heat and Mass Transfer*, Vol. 37, pp. 361-9.

Vafai, K. and Etterfagh, J. (1990), "The effects of sharp corners on buoyancy-driven flows with particular emphasis on outer boundaries", *International Journal of Heat and Mass Transfer*, Vol. 33 No. 10, pp. 2311-28.

Vierendeels, J., Merci, B. and Dick, E. (2003), "Benchmark solutions for the natural convective heat transfer problem in a square cavity with large horizontal temperature differences", *International Journal of Numerical Methods for Heat Fluid Flow*, Vol. 13 No. 8, pp. 1507-78.

Wong, J.C.F. (2007), "Numerical Simulation of two-dimensional laminar mixed-convection in a lid-driven cavity using the mixed finite element consistent splitting scheme", *International Journal of Numerical Methods for Heat and Fluid Flow*, Vol. 17 No. 1, pp. 46-93.

Wright, J.L., Jin, H., Hollands, K.G.T. and Naylor, D. (2006), "Flow visualization of natural convection in a tall, air-filled vertical cavity", *International Journal of Heat and Mass Transfer*, Vol. 49 Nos. 5-6, pp. 889-904.

Yoo, S., Park, J. and Chung, M. (2003), "Local Heat Transfer Characteristics in Simulated Electronic Modules", *Journal of Electronic Packaging, Transactions of the ASME*, Vol. 125, pp. 362-8.

Yu, Z.Z. and Harvey, T. (2000), "The precision-engineered heat pipe for cooling Pentium II in Compact PCI design", *Proceedings of the ITHERM 2000, The Seventh Intersociety Conference on Thermal and Thermomechanical Phenomena in Electronic Systems, Las Vegas*, pp. 102-5.

Further reading

Versteeg, H.K. and Malalasekera, W. (1995), *An Introduction to Computational Fluid Dynamics: Finite Volume Method*, Longman Scientific and Technical, New York, NY.

Corresponding author

B.S. Yilbas can be contacted at: bsyilbas@kfupm.edu.sa